A novel cathode for alkaline fuel cells based on a porous silver membrane

F. Bidault, A. Kucernak*

Department of Chemistry, Imperial College London, UK

ABSTRACT

Porous silver membranes were investigated as potential substrates for alkaline fuel cell cathodes and as an approach for studying pore size effects in alkaline fuel cells. The silver membrane provides both the electrocatalytic function, mechanical support and a means of current collection. Relatively high active surface area ($\sim$0.6 m^2 g^{-1}) results in good electrochemical performance ($\sim$200 mA cm^{-2} at 0.6 V and $\sim$400 mA cm^{-2} at 0.4 V) in the presence of 6.9 M KOH. The electrode fabrication technique is described and polarization curves and impedance measurements are used to investigate the performance. The regular structure of the electrodes allows parametric studies of the performance of electrodes as a function of pore size. Impedance spectra have been fitted with a proposed equivalent circuit which was obtained following the study of impedance measurements under different experimental conditions (electrolyte concentration, oxygen concentration, temperature, and pore size). The typical impedance spectra consisted of one high frequency depressed semi-circle related to porosity and KOH wettability and one low-frequency semi-circle related to kinetics. A passive air-breathing hydrogen–air fuel cell constructed from the membranes in which they act as mechanical support, current collector and electrocatalyst achieves a peak power density of 50 mW cm^{-2} at 0.40 V cell potential when operating at 25 °C.

© 2009 Elsevier B.V. All rights reserved.

1. Introduction

Recently, there has been a resurgence of interest in alkaline fuel cells (AFCs) [1–4]. Since AFCs do not require precious metal catalysts, they have the potential for lower cost mass production, compared to the other main low temperature fuel cell technology, the proton exchange membrane fuel cells (PEMFCs) [5]. AFCs can be constructed with a liquid [6] or solid electrolyte [7] using gas diffusion electrodes. Special attention on the cathode is required because it is where most of the cell performance losses occur [8]. AFC cathodes usually consist of several PTFE-bonded carbon layers applied onto a metal mesh which is used as the current collector. The catalyst is commonly supported on a high surface area carbon substrate [9,10]. The oxygen reduction reaction in alkaline media is more facile than in acid media, making the use of less expensive catalyst materials in place of platinum possible [11].

Silver has the highest electrical conductivity of any element and is approximately 100 times less expensive than platinum. Moreover, silver is one of the most active catalysts for the oxygen reduction reaction (ORR), even competitive to Pt in high concentration alkaline media [12,13]. Oxygen cathodes loaded with Ag

have also shown a longer lifetime over Pt based cathodes (3 years compare to 1 year for Pt) under practical chlor-alkali electrolysis conditions [14]. The impregnation of Ag onto carbon support via the *in situ* reduction of AgNO$_3$ has been shown to produce very fine catalyst particles, resulting in the high surface area catalyst required for optimal cathode performance [15]. Another way to obtain high surface area silver catalyst is the Raney approach, which involves leaching aluminium out of a 50% aluminium/50% silver alloy using KOH [16].

The properties of silver present opportunities for the development of new electrode designs. The authors have previously shown how silver plated nickel foam can be used as an effective electrode substrate [17]. The silver plated foam provided improved current collection compare to bare nickel foam; however, the catalytic activity was limited due to the low surface area of the open cell structure of the foam.

Porous silver membranes are mainly used in a variety of filtration applications where the antimicrobial and antibacterial properties of silver make silver membranes a very efficient filtration system [18–22]. Silver membranes are available with small pore size (micron range) and high porosity, resulting in high surface area structures. These properties are particularly useful in AFCs in which silver membranes can provide catalyst, mechanical support and a means of improved current collection compare to nickel mesh (silver having the highest electrical and thermal conductivity of all metals). Porous silver membranes offer the potential for a new cathode design that does not use a carbon support. This is benefi-

* Corresponding author at: Imperial College, Department of Chemistry, Room 433, C1, South Kensington Campus, London SW7 2AZ, UK. Tel.: +44 020 7594 5831.
E-mail addresses: anthony@imperial.ac.uk, a.kucernak@imperial.ac.uk
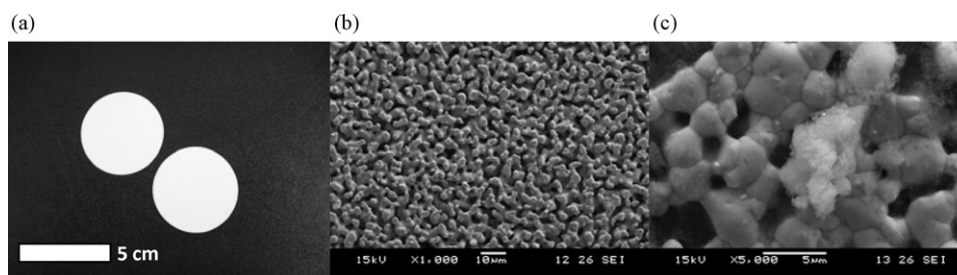(A. Kucernak).

Fig. 1. (a) Optical image of silver membranes; scanning electron microscope image showing the porous structure of silver membranes without (b) and with PTFE (c).

cial since the commonly used carbon supports degrade in alkaline media, so affecting fuel cell lifetime [9].

The aim of this work is to investigate a new cathode design for AFCs that is based on a silver membrane. The high surface area of the membrane and the catalytic activity of the silver are a promising combination for high performance. Furthermore, the ability to obtain membranes with uniform pore sizes for a range of different pores sizes allows parametric studies of pore size on other important parameters. To our knowledge, its use in fuel cells has not been investigated.

2. Experimental

2.1. Electrode preparation

Silver metal membranes from Sterlitech (Purity: 99.97%, of 50 μm nominal thickness) were used as cathode substrates (Fig. 1). The pore size of the membranes ranges from 0.2 to 5.0 μm.

Hydrophobization of the membranes was achieved using poly-tetrafluoroethylene (PTFE) solution (60 wt.% dispersion in water) from Sigma–Aldrich which was applied by pipette directly onto one side of the membrane. The PTFE deposition was applied in a two step process. In the first PTFE deposition, a loading is applied that penetrates into the membrane body, this is allowed to dry at room temperature. In the second PTFE deposition, a second amount of PTFE is applied to the membrane, but this second amount does not penetrate into the membrane but stays on the membrane surface. The electrode was then sintered in air at 320 °C for 30 min. For membranes with pore size smaller than 0.8 μm, it was found that the PTFE during the first deposition did not tend to enter the structure and remained on the surface forming a non-porous layer after sintering. It was necessary to remove this compliant film covering the membrane in order to allow gas access to the silver membrane.

The electrolyte used in all experiments was a concentrated potassium hydroxide solution (30 wt.%) if not specified otherwise prepared from 19 MΩ cm deionised water (Millipore) and Analar grade KOH pellets (VWR).

2.2. Electrode characterization

Electrochemical and impedance measurements (frequency range: 10 kHz to 0.1 Hz, amplitude 0.02 V_{rms}) were performed using a PGSTAT30 potentiostat (Autolab, EcoChemie, Netherlands). All the results presented in this paper are three electrode measurements using a dynamic hydrogen reference electrode from Gaskatel (Hydroflex HREF B01). All electrochemical potentials are henceforth referred to this electrode.

The surface of the silver membranes was analysed using a scanning electron microscope (JEOL JSM-5610LV).

The catalytic activity of the various silver membranes were measured in a half-cell configuration using a three electrode set-up and a Luggin capillary situated less than 0.5 mm from the electrode surface and a counter electrode of nickel foam which was 10 times the geometrical surface area of the working electrode, to avoid exces-

sive polarization. Silver membrane cathodes (1 cm^2) were floated on the surface of a fresh KOH solution with the other side exposed to an oxygen or air atmosphere through forced convection [23]. Cathodes were polarized after 15 min in contact with the electrolyte under oxygen in a first scan (0.01 V s^{-1}) from OCV (1.1 V) to 0.1 V for conditioning. All polarization curves shown are the results of a second scan. A third scan was then taken (not shown in this paper) to make sure that the optimum performance was obtained. Impedance spectra were then taken at 0.8 V, still under oxygen. Finally, measurements were taken under air.

2.3. Fuel cell operation

Cathodes were tested in a cylindrical 4 cm^2 hydrogen–air fuel cell utilising 25 mm diameter silver membrane disks as mechanical support, current collector and catalyst. The fuel cell was constructed using a commercial hydrogen reformate anode from Alfa Aesar (Johnson Matthey Company, 0.4 mg cm^{-2} Pt, Toray paper GDL) separated from the cathode with a plastic mesh (1 mm thick). Current was collected around the edge of the silver membrane disk, requiring that the current from the centre of the disk flowed >1 cm to the external current collector. The KOH solution was 30 wt.%, pure hydrogen (99.999%) from BOC was provided on the anode side whereas the cathode side was left open to the laboratory air in self-breathing mode without any supplemental gas flow. As the cathode was open to the laboratory air, no backpressure control was possible. Utilising optimised PTFE loading, the fuel cell did not show any weeping of electrolyte on the cathode side. Fuel cell results are not iR corrected.

3. Results and discussion

3.1. Characterization of silver membranes

Table 1 summarizes results of different measurements made on the different silver membranes. The particle retention characteristic is taken from the manufacturer's data sheet, and may be broadly considered to be close to the pore diameter. The porosity was calculated by weighing a known geometric volume of membrane knowing the density of pure silver. The specific surface area calculated using Eq. (1) relates to an estimation of the surface area considering only the inside of each pore which is assumed to be

Table 1
Key characteristics of silver membranes.

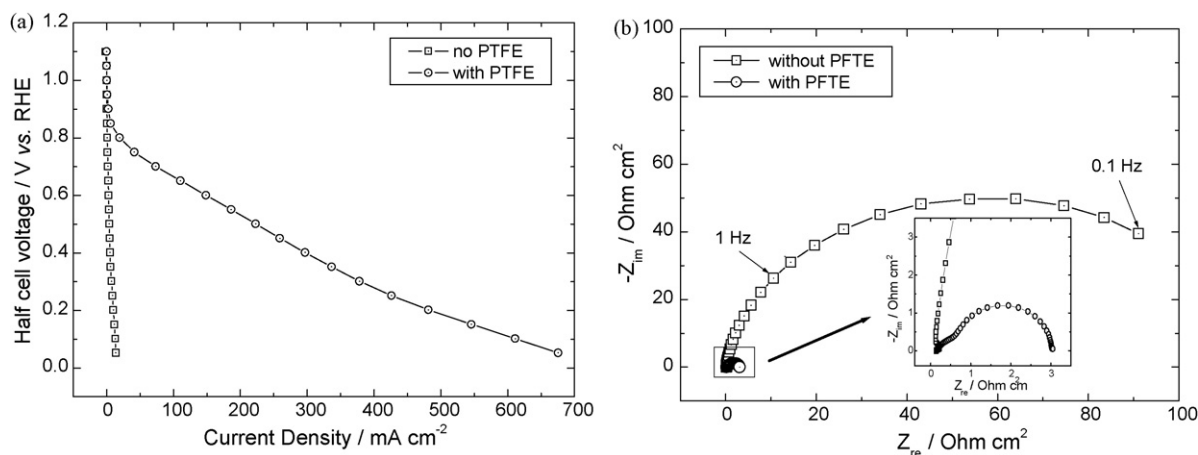| Particle retention/μm	Thickness/μm	Porosity/%	Specific surface area/m^2 g^{-1}
0.2	57	26.1	0.67
0.45	57	33.6	0.43
0.8	85	54.2	0.56
1.2	83	56.4	0.41
3	95	56.8	0.17
5	92	51.2	0.08

Fig. 2. Polarization curves and impedance results for cathodes made of silver membrane (1.2 μm) with and without PTFE (12.3 mg cm^{-2} total amount deposited) under oxygen at 20 °C in 30 wt.% KOH solution (a). Polarization results; (b) impedance measurements at 0.8 V (cell voltage) from 10 kHz to 0.1 Hz. Inset is the same plot scaled to show the details of the scans at low Z.

a long cylinder (tortuosity = 1) where P is the membrane porosity, ρ the silver density and r is the radius of the cylinder. It can be seen that silver membranes with 0.2 and 0.8 μm have the highest estimated surface area and therefore should give the best performance. This model provides only an approximate assessment of the specific surface area as clearly the tortuosity of the membranes is greater than one (Fig. 1).

$$A = \frac{2P}{\rho r (1 - P)} \tag{1}$$

SEM images of the silver membrane surface (0.8 μm) before and after PTFE deposition are shown in Fig. 1(b),(c). As can be seen in Fig. 1b, the porosity of the membrane appears to be homogeneous with pores in the micron range. In Fig. 1c, an excess of PTFE can be seen in the centre of the picture with smaller particles in the membrane pores.

3.2. Characterization of silver membranes cathodes

A silver membrane (1.2 μm) cathode was prepared with a PTFE coating following the procedure described in Section 2. The half-cell polarization curves of a cathode with PTFE and a cathode without PTFE coating under oxygen clearly demonstrate the importance of the PTFE coating to obtain good performance (Fig. 2a).

Impedance measurements were performed on cathodes prepared with and without PTFE (Fig. 2b). As can be seen, the cathode without PTFE exhibits a single large capacitive arc whereas the cathodes made with PTFE (Fig. 2b, inset) shows a depressed arc at high frequency and a capacitive semi-circle at low frequency which are much smaller than for the cathode without PTFE. It is believed that the structure of the cathode without PTFE is completely flooded with electrolyte, making the mass transport resistance very high. The PTFE coating keeps the gas side of the electrode free of KOH solution which greatly improves the reactant gas accessibility, so decreasing the mass transport resistance.

The same PTFE treatment was applied to silver membranes with different pore sizes with a target PTFE loading of 13 mg cm^{-2}, and the resulting polarization curves and impedance results are shown in Fig. 3. As can be seen for the polarization results, Fig. 3a, the best performance was obtained for silver membranes with 0.8 and 1.2 μm pore size. The difference in surface area is obviously part of the reason for the improvement in performance for these electrodes
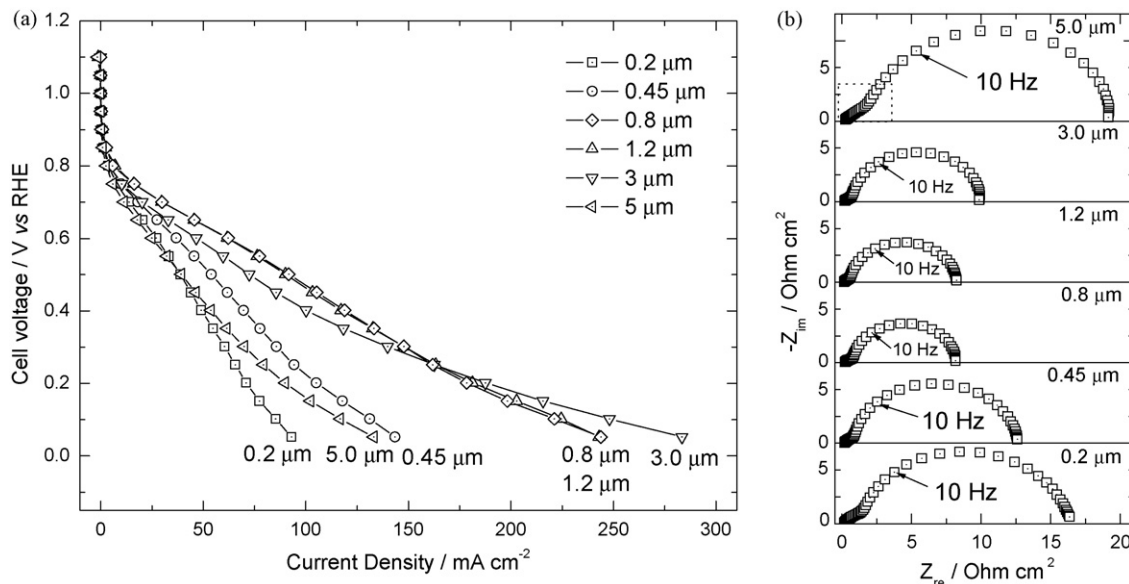

Fig. 3. Polarization curves (a) and impedance measurements (b) of cathodes made of silver membranes with different pore sizes under air at 20 °C in 30 wt.% KOH solution.
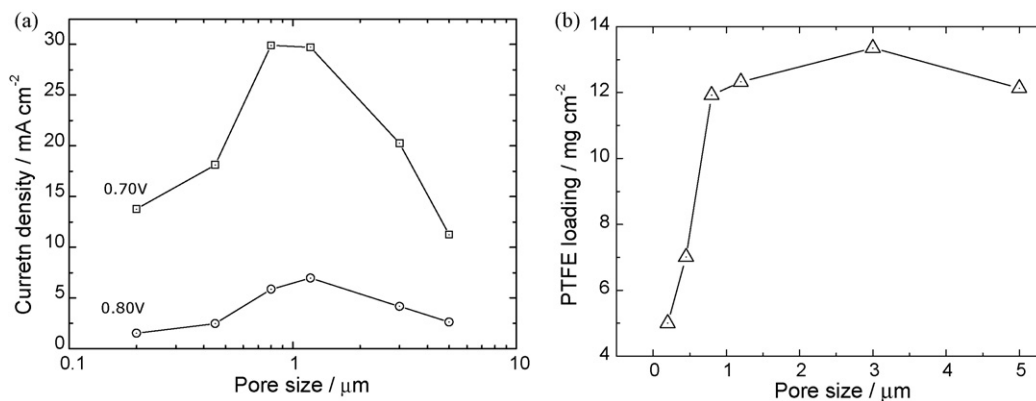
Fig. 4. Current density at 0.70 and 0.80 V (a) [data taken from Fig. 3(a)]; and PTFE loading (b) as a function of membrane pore size for a consistently applied PTFE treatment.

but more importantly the PTFE loading seems to be important for optimising performance (see below).

Impedance measurements were performed on these cathodes, the results of which are shown in Fig. 3b. All the cathodes share the same impedance spectra features, with a depressed high frequency arc and a low-frequency capacitive semi-circle. The decrease in size of the low-frequency semi-circle on membranes with pore sizes between 0.2 and 1.2 μm is believed to be due to the increase in PTFE loading whereas its increase in size with membrane between 1.2 and 5 μm pore size is believed to be related to the decrease in surface area since the PTFE loading is similar for these cathodes. The best performing cathodes (0.8 and 1.2 μm) show the smallest low-frequency semi-circle which is believed to be due to the fact that 0.8 and 1.2 μm pore size are both optimal if considering surface area and PTFE. For this reason, only these two types of membrane are considered in the following.

Indicative performance of the cathodes at two relevant potentials (0.70, 0.80 V) extracted from Fig. 3(a) is shown in Fig. 4(a). An improvement in performance with decreasing pore size is seen down to a pore size of 0.8 μm, although for smaller pores, there is a decrease in performance. As pore size decreases, the specific surface area of the membrane tends to increase (Table 1), and so we might expect performance to be highest for the smallest pore size, however this is not the case. Even though a consistent application technique was used, it was found that the PTFE loading for the different membranes was not the same (Fig. 4b). Apparently, the inferior results from membranes with 0.2 and 0.45 μm pore sizes (Fig. 4a) can be explained by the poor PTFE loading after the hydrophobization step (see Section 2). This could be due to the fact that the 0.2 and 0.45 μm membranes would have pores too

small to allow PTFE particle infiltration, preventing the formation of hydrophobic areas within the membrane. It is to be noted that improved performance for the 0.2 and 0.45 μm membranes compared to the 0.8 and 1.2 μm membranes would be expected because of the increase in specific surface area were it possible to obtain a suitable PTFE coating.

3.3. Assessment of performance variation under different conditions

In order to attribute physical significance to the features observed in the impedance spectra, measurements were taken under different experimental conditions using a 1.2 μm pore size silver membrane cathode (total PTFE loading: 12.3 mg cm^{-2}). Fig. 5(a) shows the impedance spectra of the cathode under air and oxygen at the same half-cell voltage (0.8 V). It can be seen that the high frequency semi-circle is unchanged, whereas the low-frequency feature is much smaller under pure oxygen. Fig. 5(b) shows the Bode phase-plot spectra of the same cathode at different cell voltages in an oxygen atmosphere. It can be seen that the high frequency semi-circle is again unchanged, whereas the size of the low-frequency semi-circle decreases when increasing the polarization. Both results demonstrate that the low-frequency semi-circle is related to kinetics (included charge transfer and mass transport) whereas the high frequency one seems to be related to the electrode structure (porosity).

Impedance spectra of the same cathode were obtained in different KOH concentration (results not presented). The low-frequency arc increases in size when the KOH concentration increases. This could be due to the fact that at higher concentrations, KOH solution
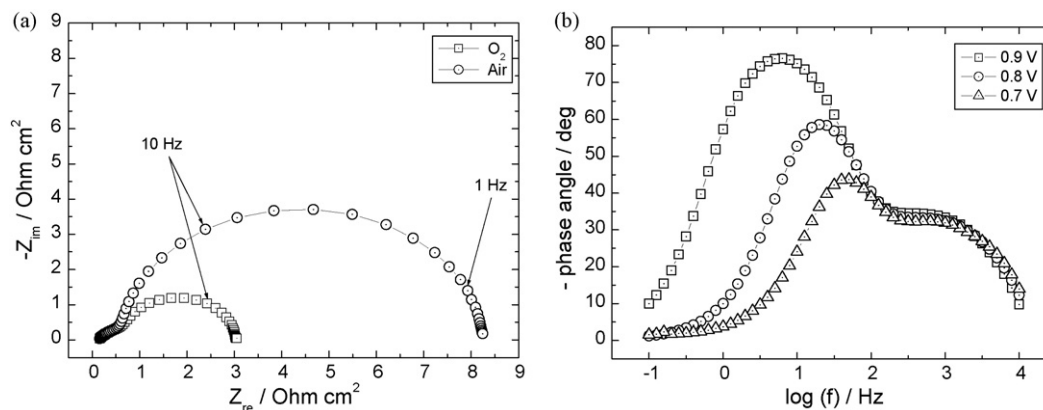

Fig. 5. Impedance measurements of silver membrane cathode (1.2 μm) at 20 °C in 30 wt.% KOH solution from 10 kHz to 0.1 Hz. (a) Nyquist plot at 0.8 V showing the effect of reactant-oxygen and air; (b) Bode phase-plot spectra under oxygen showing the effect of polarization potential.
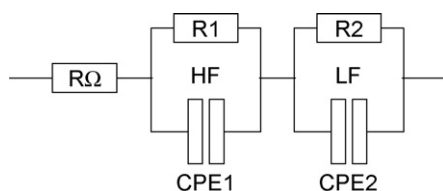
Fig. 6. Equivalent circuit of the silver membrane cathode used to fit both the high frequency and low semi-circles.

Table 2
Fitted values of equivalent circuit parameters of the high frequency semi-circle for silver membrane cathode in different KOH concentration.

KOH concentration/%	$R\Omega/\Omega$	$R1/\Omega$	CPE1	
			Y_1	n
10	0.516	2.14	1.14	0.56
20	0.342	1.96	1.63	0.56
30	0.290	1.77	2.32	0.52

penetrates deeper into the membrane structure which hinders the reactant gas accessibility increasing the mass transport resistance.

$R\Omega$ and the first constant phase element from equivalent circuit shown in Fig. 6 was used to fit the high frequency semi-circles. A constant phase element (CPE) is introduced because the semi-circles show some depression which relates to the lack of homogeneity of the electrode capacitance [24]. The impedance of a constant phase element is given by:

$$Z_{CPE} = \frac{1}{Y_0(j\omega)^n} \qquad (2)$$

where Y_0 is the admittance relating to the double-layer capacitance and n is a constant between -1 and 1 giving information about the nature of the CPE. When $n = 1$, Y_0 corresponds to the ideal capacitance C and the CPE behaves as a capacitance.

As can be seen in Table 2, $R\Omega$ decreases when the KOH solution concentration increases (increase of the electrolyte conductivity) which was expected because $R\Omega$ represents the Ohmic resistances of the electrolyte in the cell. Surprisingly, $R1$ appears to decrease with the increase of the electrolyte concentration. If $R1$ was only a structural (physical) related resistance, it should stay constant
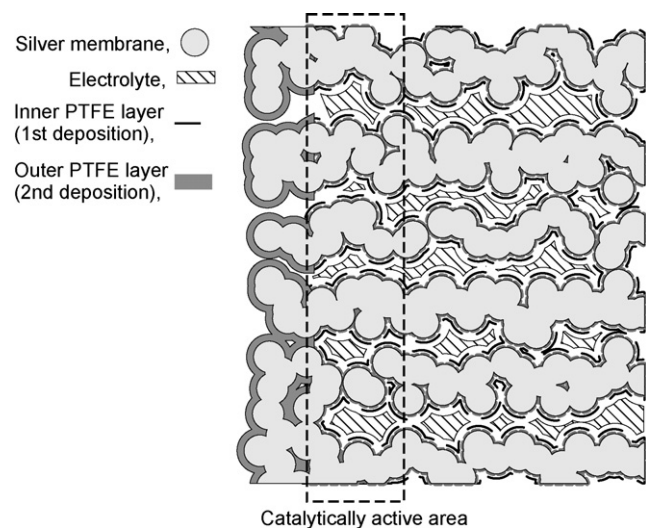

Fig. 7. Cartoon showing the deposition of PTFE on the silver membrane and how this may affect wetting of the electrolyte. The first PTFE layer is deposited throughout the entire membrane structure whereas the second deposition occurs only on the surface. The catalytically active area immediately beneath the outer PTFE layer is highlighted.
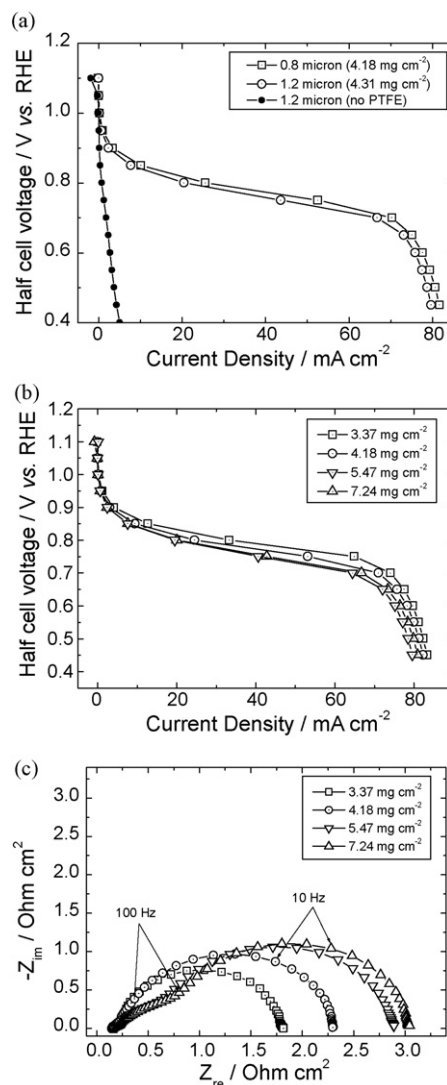

Fig. 8. Effect of PTFE loading within the membrane under oxygen at 20 °C in 30 wt.% KOH solution. (a) Polarization curve showing pore size effect for constant PTFE loading from the first deposition step. (b) Polarization curves for 0.8 μm silver membranes showing the effect of the PTFE loading from the first deposition step; (c) impedance spectra for the membranes in (b) obtained at 0.8 V (cell voltage) from 10 kHz to 0.1 Hz. Effect of first PTFE deposition step on silver membrane performance under oxygen at 20 °C in 30 wt.% KOH solution. No second PTFE deposition step was performed. (a) Polarization curve showing pore size effect for constant PTFE loading from the first deposition step. (b) Polarization curves for 0.8 μm silver membranes showing the effect of the PTFE loading from the first deposition step; (c) impedance spectra for the membranes in (b) obtained at 0.8 V (cell voltage) from 10 kHz to 0.1 Hz.

which is obviously not the case. The admittance of the constant phase element, representing the double-layer, also increases when the KOH concentration increases; this could again be due to the deeper KOH penetration into the electrode structure with greater KOH concentration. The low value of the parameter n (~0.5) suggests that the electrode consists of semi-infinite pores [25] and is in agreement with porosity effects [26].

Impedance spectra of the same cathode were obtained at constant KOH concentration but different temperatures (results not presented). The low-frequency semi-circle decreased when the temperature increased, which is expected since it is related to kinetics. The high frequency semi-circle also decreased when the electrolyte temperature increased. From both electrolyte concentration and temperature dependence studies, we can conclude that $R1$ is strongly related to the electrolyte conductivity.
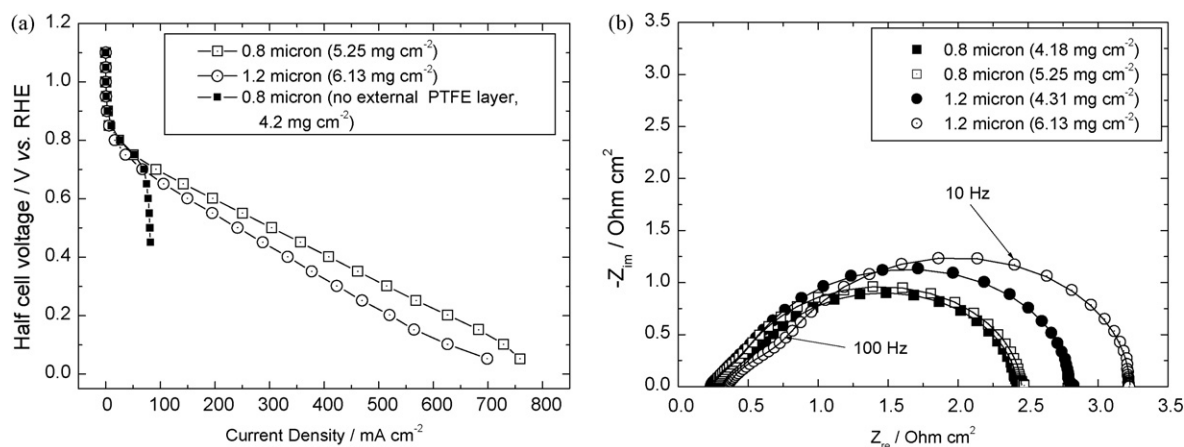
Fig. 9. Polarization curves, (a) and electrochemical impedance results (b) for cathodes made of silver membrane (0.8 and 1.2 μm) with optimised 1st and 2nd PTFE loadings under oxygen at 20 °C in 30 wt.% KOH solution. Impedance data obtained at 0.8 V, from 10 kHz to 0.1 Hz (symbol: experimental data, line: fit). Performance of silver membranes after optimised first and second PTFE deposition steps. Polarization curves showing optimised 0.8 and 1.2 μm pore electrodes and for comparison a 0.8 μm pore size electrode with only the optimised first PTFE loading, (a). Electrochemical impedance results for cathodes made of silver membranes (0.8 and 1.2 μm) under oxygen at 20 °C in 30 wt.% KOH solution, (b). Impedance data obtained at 0.8 V, from 10 kHz to 0.1 Hz (symbol: experimental data, line: fit). Total PTFE loadings are displayed for each electrode (first PTFE deposition step leads to a loading of 4.2 ± 0.1 mg cm^{-2}).

The equivalent circuit shown in Fig. 6 is then proposed to fit the silver membrane cathodes impedance spectrum where $R\Omega$ is the sum of electrolyte resistance (bulk), contact resistances and cell resistances; $R1$ is the Ohmic drop resistance of the electrolyte in active pores (or flooded pores) which depends on electrode porosity and wettability and finally $R2$ is related to kinetics. Similar circuits have already been proposed in the case of cathode [27] and anode [28] in alkaline media.

3.4. Optimisation of PTFE loading

As described in Section 2, PTFE was deposited twice on the membranes. In the first step, the PTFE dispersion penetrates throughout the entire membrane volume. In the second deposition step, the PTFE is only deposited on the surface of the membrane. The ability to tailor the PTFE distribution both within the membrane and on the membrane surface is crucial to obtaining good performance. A cartoon of the expected resultant configuration, in which a greater loading of PTFE is on the surface than in the body of the silver membrane is shown in Fig. 7.

In order to study this effect, we initially measured the performance of the two best performing membranes from Fig. 3a (0.8, 1.2 μm) after only the *first PTFE deposition* with a target loading of 4 mg cm^{-2} (Fig. 8a). The benefit of including this PTFE treatment is clearly seen for the 1.2 μm membrane compared to the same membrane with no PTFE. The cathode made with 0.8 μm pore size outperforms the one made with 1.2 μm pore size for the same PTFE loading. It is also clear why the second PTFE deposition step is important, as in its absence a significant mass transport limitation is seen at current densities of $j > 70$ mA cm^{-2}.

In order to optimise the first PTFE deposition step we looked at the performance of the 0.8 μm pore size silver membrane as a function of the PTFE loading in the first step (Fig. 8b). In order to

assess only the effect of PTFE loading within the membrane, the second PTFE deposition (i.e. deposition of PTFE on the membrane surface) was not performed. For this reason the performance at high current density ($j > 70$ mA cm^{-2}) is poor. As can be seen in Fig. 8b, although PTFE is required in the inner structure its loading should be kept low because performance decreases when the PTFE loading is increased. As expected, the size and shape of the high frequency semi-circle change with PTFE loading. It is more marked with higher PTFE loadings (Fig. 8c).

Having determined the optimum first loading value (i.e. the amount of PTFE dispersed throughout the entire membrane volume), we also optimised the second PTFE amount (i.e. the amount of PTFE deposited on the membrane surface). Fig. 9a shows the resultant polarization curves for two different pore size membranes (0.8 and 1.2 μm) utilising a first PTFE loading of 4.2 ± 0.1 mg cm^{-2}. The PTFE loading displayed in Fig. 9 is the total PTFE loading (i.e. first + second PTFE loading). The effect of the second PTFE treatment is to remove the mass transport limitation seen at about 80 mA cm^{-2} for electrodes which only have the first (internal) PTFE treatment. Performance of the 0.8 μm cathodes are quite good with 196 mA cm^{-2} at 0.6 V and 408 mA cm^{-2} at 0.4 V, considering the fact that it is a very simple electrode design.

In Fig. 9b, impedance measurements of the same cathodes can be seen. The experimental data (symbols) are well fitted (lines) with the equivalent circuit shown in Fig. 6. Results are summarized in Table 3. The double-layer capacities of porous electrodes are proportional to their wetted areas. Y_1 (larger than Y_2) would be representative of the total flooded area of the cathode, whereas Y_2 would be representative of the catalytic active surface area of the cathode which is believed to be located just below the PTFE coating as seen in Fig. 7. It can be seen that the higher the PTFE loading, the lower Y_1. This is expected because less electrolyte floods the electrode structure which means a decrease of the double-layer

Table 3
Fitted values of equivalent circuit parameters (Fig. 6) for curves in Fig. 9(b).

Electrode pore size/μm	PTFE loading/mg cm^{-2}	$R\Omega/\Omega$	$R1/\Omega$	CPE1		$R2/\Omega$	CPE2	
				Y_1	$n1$		Y_2	$n2$
0.8	4.18	0.321	0.255	1.10	0.78	1.849	0.627	0.96
0.8	5.25	0.248	0.238	0.985	0.81	1.968	0.627	0.97
1.2	4.31	0.233	0.322	0.982	0.77	2.254	0.458	0.98
1.2	6.13	0.358	0.471	0.553	0.80	2.399	0.476	0.99

Table 4
Estimates of the electrode surface area and double-layer capacitance from impedance data in Fig. 9.

Silver membrane pore size/μm	Estimated surface area/m^2 g^{-1}	Estimated double-layer capacitance/F cm^{-2}
0.8	0.56	0.60
1.2	0.41	0.47

capacitance. The PTFE loading does not have much effect on Y_2 and $R2$ for both pore size cathodes because these parameters are related to the active surface area which is believed to vary mostly with the structure of the membrane (pore size, roughness of the surface, etc.) but not much with the penetration depth of the PTFE (or loading) in the pore (considering the pore as a long cylinder).

In the same way, $R1$ and $R2$ are lower (Y_1 and Y_2 are higher) for the 0.8 μm pore size cathode than for the 1.2 μm case. This is because the surface area of the 0.8 μm cathode is higher than that of the 1.2 μm cathode. This increases the surface of the membrane in contact with the electrolyte decreasing $R1$ and $R2$ and increasing Y_1 and Y_2.

The double-layer capacitances were estimated by the means of Eq. (3) [28,29] using data listed in Table 3. Results of Eqs. (1) and (3) are shown in Table 4 where it can be seen that the surface area of the 0.8 μm pore size electrode is higher than the 1.2 μm pore size electrode; this explains the superior performance for the 0.8 μm electrode. It is interesting to note that both results are in good accordance.

$$C_{dl} = \left(\frac{C_2}{((R_\Omega + R_1)^{-1} + R_2^{-1})^{(1-n_2)}} \right)^{1/n_2} \tag{3}$$

In order to study the stability of the cathode, 10 successive polarization scans have been performed (after the 3 first scans) following immediately after by impedance measurement at 0.8 V (data not shown). A decay of current density at different voltages was observed. The current density at each voltage decreased with the number of scan; the higher the polarization the higher the decrease in current density. The equivalent circuit shown in Fig. 8 was used to fit the impedance spectra obtained after each scans (not shown). $R\Omega$ and $R1$ increased slightly with the number of scan whereas Y_2 was relatively stable. $R2$ and Y_1 increased significantly with scan number. The increase in Y_1 is believed to be due to increased flooding of the membrane structure. This hinders gas accessibility increasing mass transport resistance which can be related to the increase in $R2$. This flooding or weeping effect is well known in liquid alkaline system and is one of the main rea-

sons for cathode performance degradation [8]. In future work we will test this cathode design with an anionic membrane as in this case no movement of the electrolyte interface is seen and a stable three-phase contact region is formed.

3.5. Testing membranes within a fuel cell

In order to improve the activity of the electrode, 10 nm of Pt was sputtered on one side of a 0.8 μm silver membrane, equivalent to a loading of 21 μg cm^{-2}, followed by the standard PTFE treatment. Two different cathodes were fabricated: in one of them the Pt coating was on the gas side and in the other the Pt coating was on the electrolyte side of the membrane. Only the cathode with the Pt coating on the gas side showed an improved performance meaning that most of the electrode structure is flooded with electrolyte and the thickness of the membrane could be greatly reduce without any effects on cathode performance. The performance of the membrane with Pt on the gas side is shown in Fig. 10a. A clear improvement can be seen with a performance of 260 mA cm^{-2} at 0.6 V and 500 mA cm^{-2} at 0.4 V. In the low current regime, 0.1 to 100 mA cm^{-2}, where the potential is dominated by electrokinetics, a 30 mV positive shift in the curve is seen. At higher current densities the improvement in performance is even greater, suggesting that mass transport to the Pt layer is enhanced compared to transport to the silver electrode. This is to be expected if the platinum layer is immediately below the outer PTFE layer.

The improvement in performance is assumed to be due to the higher catalytic activity of Pt compared to Ag. This was confirmed by electrochemical impedance spectroscopy (Fig. 10(a), inset) for which only the low-frequency kinetic semi-circle was seen to reduce in size when Pt was introduced onto the cathode. Tafel analysis of the polarization curves in the kinetic region ($E > 0.8$ V) gives a slope of 105 mV dec^{-1} for Ag and 93 mV dec^{-1} for the Pt on Ag electrode.

Testing of the new cathode in a 4 cm^2 cylindrical hydrogen–air fuel cell was also performed to see if good results could be obtained utilising the silver membrane (0.8 μm pore size) with 10 nm of Pt (21 μg cm^{-2}) as cathode. Under these conditions the silver mem-
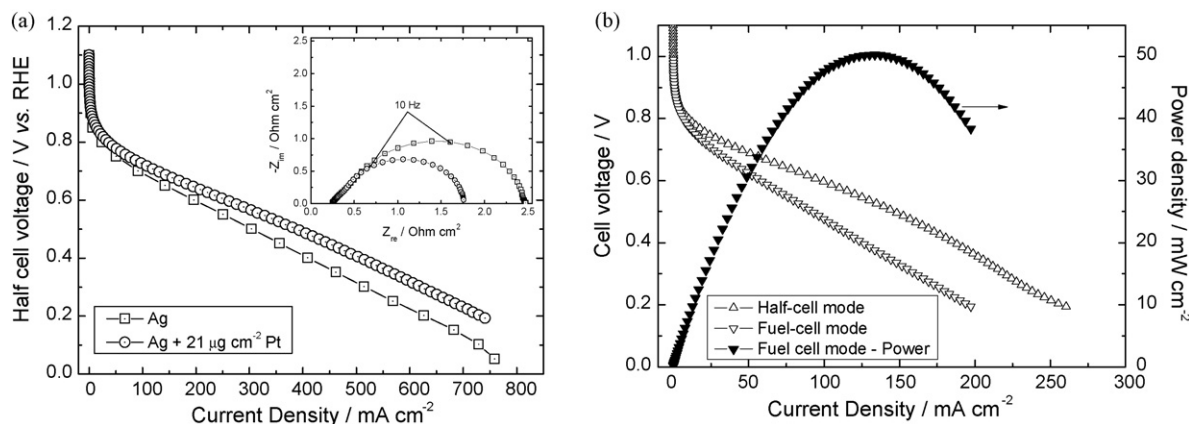

Fig. 10. (a) Half-cell polarization curves of cathodes made of silver membrane (0.8 μm) and silver membrane with 10 nm of Pt (20 μg cm^{-2}) under oxygen at 20 °C. Inset – electrochemical impedance spectroscopy of each electrode at 0.90 V from 10 kHz to 0.1 Hz. (b) Hydrogen–air fuel cell test of silver membrane with 10 nm of Pt (21 μg cm^{-2}) utilising 30 wt.% KOH solution as electrolyte and 1 mm electrode separation. Pt on carbon paper (0.4 mg cm^{-2}) used as anode. For comparison, the same cathode operating under half-cell operation in the same cell is shown.

brane functions as both mechanical support, sole current collector (>1 cm maximum current path), and electrocatalyst. We were able to show good performance of the fuel cell utilising our optimised PTFE loading with the cathode open to the air (i.e. without any backpressure), and without weeping of the electrolyte through the cathode membrane. For comparison, the cathode was also tested potentiostatically in the same cell and under the same conditions (passive air-breathing mode). As can be seen from Fig. 10b, performance of the fuel cell is slightly reduced compared to the results obtained in the half-cell configuration, yet still attain a peak power of 50 mW cm^{-2} at a cell voltage of 0.4 V under passive self-breathing operation. This is an impressive performance considering that no backpressure or forced air convection is applied, and the cathode is open to the laboratory air. The reduction in performance compared to the half-cell results could be explained by the presence of the spacer between the cathode and the anode. Comparison of impedance spectra (not shown) did not show any increase in Ohmic resistance between the half-cell and fuel cell mode but an increase in the low-frequency kinetic semi-circle. This could be due to the higher resistance to species (H_2O, OH^-) to migrate from anode to cathode induced by the spacer (since there was no difference in air flow rate or electrode structure).

The silver loading of the new cathode design (using a membrane with 0.8 μm pores) is estimated at 45 mg cm^{-2}. Such a loading has been used before in test cathodes for alkaline fuel cells. For instance, Wagner et al. utilised 0.4 mm thick electrodes with a silver loading of greater than 47 mg cm^{-2} to study the longevity of electrode performance [30]. In our case the electrodes are only ~85 μm thick, 1/5th of those mentioned above. This reduction of thickness may be beneficial for the transport properties of gases. Indeed, we estimate that the membranes could be reduced to maybe 20 μm thickness whilst retaining mechanical stability. In such a case, the loading would be reduced by a factor of 4 with a total cost of 100 \$ m^{-2} for combined electrocatalyst + current collector + mechanical support which is not far away from the cost of nickel mesh alone (60 \$ m^{-2}) in the conventional design – to which would still have to be added the cost of the electrocatalyst.

4. Conclusion

Porous silver membranes, which are commonly used as filter membranes in diverse chemical processes, have been successfully demonstrated as substrates for fuel cell cathodes in alkaline media. These membranes are useful as they have a consistent structure which allows parametric analysis of a wide range of variables whilst keeping the general structure of the electrode constant. Hence it has been possible to test pore size effects in a way which is much more difficult to achieve using standard electrodes. A treatment process, consisting of the application of PTFE dispersion both within and on one side of the electrode, is necessary to obtain good electrochemical performance. The PTFE loading has been optimised to

get optimal results from the porous silver structure in a two step process which is necessary to avoid any mass transportation limitation. The membrane with 0.8 μm pore size appeared to be the more adequate for high performance because of its high surface area. Performance obtained are quite good with 196 mA cm^{-2} at 0.6 V and 408 mA cm^{-2} at 0.4 V and with 260 mA cm^{-2} at 0.6 V and 500 mA cm^{-2} at 0.4 V under oxygen using a very thin (10 nm) Pt coating on top of the Ag. Utilised in passive air-breathing mode, a hydrogen–air fuel cell utilising the above-mentioned platinum on silver cathode attains a power density of 50 mW cm^{-2} at a cell potential of 0.4 V utilising the silver membrane also as mechanical support and current collector.

References

[1] M. Duerr, S. Gair, A. Cruden, J. McDonald, Journal of Power Sources 171 (2007) 1023–1032.
[2] T. Hejze, J.O. Besenhard, K. Kordesch, M. Cifrain, R.R. Aronsson, Journal of Power Sources 176 (2008) 490–493.
[3] G. Mulder, P. Coenen, A. Martens, J. Spaepen, International Journal of Hydrogen Energy 33 (2008) 3220–3224.
[4] I. Verhaert, M. De Paepe, G. Mulder, Journal of Power Sources 193 (2009) 233–240.
[5] G.F. McLean, T. Niet, S. Prince-Richard, N. Djilali, International Journal of Hydrogen Energy 27 (2002) 507–526.
[6] K. Strasser, Journal of Power Sources 29 (1990) 149–166.
[7] J.R. Varcoe, Electrochemistry Communications 8 (2006) 839.
[8] F. Bidault, D.J.L. Brett, P.H. Middleton, N.P. Brandon, Journal of Power Sources 187 (2009) 39–48.
[9] M. Cifrain, K.V. Kordesch, Journal of Power Sources 127 (2004) 234–242.
[10] K Tomantschger, F. McClusky, L. Oporto, A. Reid, K. Kordesch, Journal of Power Sources 18 (1986) 317–335.
[11] B.B. Blizanac, P.N. Ross, N.M. Markovic, Electrochimica Acta 52 (2007) 2264–2271.
[12] M. Chatenet, L. Genies-Bultel, M. Aurousseau, Journal of Applied Electrochemistry 32 (2002) 1131–1140.
[13] V Hacker, E. Wallnofer, W. Baumgartner, T. Schaffer, J.O. Besenhard, H. Schrottner, M. Schmied, Electrochemistry Communications 7 (2005) 377–382.
[14] N. Furuya, H. Aikawa, Electrochimica Acta 45 (2000) 4251–4256.
[15] K. Smrcek, J. Beran, J. Jandera, Journal of Power Sources 2 (1978) 273–286.
[16] M. Al-Saleh, Journal of Applied Electrochemistry 24 (1994) 575–580.
[17] The effect of continuously changing potential on the silver electrode in alkaline solutions, The Journal of Physical Chemistry 63 (1959) 107–110.
[18] O. Akhavan, E. Ghaderi, Current Applied Physics 9 (2009) 1381–1385.
[19] S.A. Glazier, Journal of Microbiological Methods 20 (1994) 23.
[20] Y. Lv, H. Liu, Z. Wang, S. Liu, L. Hao, Y. Sang, D. Liu, J. Wang, R.I. Boughton, Journal of Membrane Science 331 (2009) 50–56.
[21] A. Pérez Padilla, Desalination 114 (1997) 203.
[22] I. Sondi, B. Salopek-Sondi, Journal of Colloid and Interface Science 275 (2004) 177–182.
[23] S. Srinivasan, Fuel Cells: From Fundamentals to Applications, Springer, 2006, pp. 692.
[24] A. Lasia, Journal of Electroanalytical Chemistry 397 (1995) 27–33.
[25] R. de Levie, Electrochimica Acta 9 (1964) 1231–1245.
[26] H. Keiser, K.D. Beccu, M.A. Gutjahr, Electrochimica Acta 21 (1976) 539–543.
[27] D. Thiele, A. Züttel, Journal of Power Sources 183 (2008) 590–594.
[28] P.-L. Cabot, F. Alcaide, E. Brillas, Journal of Electroanalytical Chemistry 626 (2009) 183–191.
[29] J. Kubisztal, A. Budniok, A. Lasia, International Journal of Hydrogen Energy 32 (2007) 1211–1218.
[30] N. Wagner, M. Schulze, E. Gulzow, Journal of Power Sources 127 (2004) 264–272.